

Analysis of one- and two-particle spectra at RHIC based on a hydrodynamical model

TETSUFUMI HIRANO^{1,5}, KENJI MORITA², SHIN MUROYA³
and CHIHO NONAKA^{4,6}

¹Physics Department, University of Tokyo, Tokyo 113-0033, Japan

²Department of Physics, Waseda University, Tokyo 169-8555, Japan

³Tokuyama Women's College, Tokuyama, Yamaguchi 745-8511, Japan

⁴IMC, Hiroshima University, Higashi-Hiroshima, Hiroshima 739-8521, Japan

⁵RIKEN BNL Research Center, Brookhaven National Laboratory, Upton, NY 11973, USA

⁶Department of Physics, Duke University, Science Drive Durham, NC 27708-0305, USA

Abstract. We calculate the one-particle hadronic spectra and correlation functions of pions based on a hydrodynamical model. Parameters in the model are so chosen that the one-particle spectra reproduce experimental results of $\sqrt{s} = 130$ A·GeV Au + Au collisions at RHIC. Based on the numerical solution, we discuss the space-time evolution of the fluid. Two-pion correlation functions are also discussed. Our numerical solution suggests the formation of the quark–gluon plasma with large volume and low net baryon density.

Keywords. Relativistic heavy-ion collisions; quark–gluon plasma; hydrodynamical model; two-particle correlations.

PACS Nos 24.10.Nz; 12.38.Mh; 25.75.Gz

1. Introduction

The new state of matter, the quark–gluon plasma (QGP), is expected to be produced in relativistic heavy-ion collisions. Though the recent experimental data of $\sqrt{s} = 130$ A·GeV Au + Au collisions at RHIC have already been presented [1], the collision process is too complicated to understand clearly due to many-body interactions and multiparticle productions. Therefore we need a simple phenomenological description as the basis for further investigation. In this talk, based on a hydrodynamical-model calculation, we try to give a possible explanation for the RHIC experimental results of the single-particle spectra and correlation function [2].

2. Model and particle spectra

Assuming that local thermal and chemical equilibrium are established, the dynamical evolution of the system can be described by a relativistic hydrodynamics. We numerically solve the hydrodynamical equations for the perfect fluid and baryon number conservation

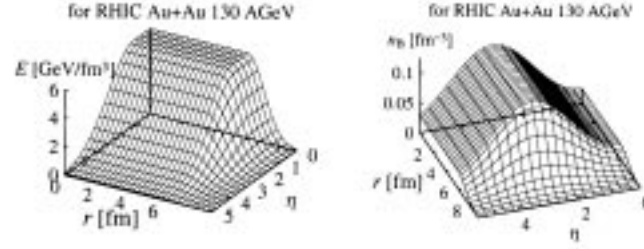


Figure 1. Left: Initial energy density distribution. Right: net baryon number distribution.

Table 1. Parameters and output from the fluid.

| | Au+Au at 130 A·GeV | Pb+Pb at 17.4 A·GeV |
|---|-------------------------|--------------------------|
| E_{\max} | 6.0 GeV/fm ³ | 5.74 GeV/fm ³ |
| n_{\max} | 0.125 fm ⁻³ | 0.7 fm ⁻³ |
| Total n_B | 132 | 305 |
| $\langle T_f \rangle$ | 125 MeV | 123 MeV |
| $\langle \mu_B \rangle$ | 76.1 MeV | 280.2 MeV |
| $\langle v_T \rangle_{ \eta \leq 0.1}$ | 0.51 | 0.467 |

with cylindrical symmetry [3], where we take both longitudinal and transverse dynamical expansion into account. We use an equation of state (EOS) with a phase transition of first order [4].

We put the initial time as $\tau = \sqrt{t^2 - z^2} = 1.0$ fm. Initial longitudinal velocity is assumed to be Bjorken's solution, $v_z = z/t$. Initial transverse flow velocity is neglected. We parametrize the initial energy density distribution and net baryon number distribution as in figure 1.

For both RHIC and SPS, we adjust the parameters in the model so that calculated single-particle spectra reproduce the experimental results. The parameter sets for both experiments are summarized in table 1.

Once the freeze-out hypersurface is fixed, one can calculate the single-particle spectra via Cooper–Frye formula. We take account of not only hadrons directly emitted from the freeze-out hypersurface but also the ones produced in the decay of resonances. Note that the resonances are also emitted from the freeze-out hypersurface. We include decay processes $\rho \rightarrow 2\pi$, $\omega \rightarrow 3\pi$, $\eta \rightarrow 3\pi$, $K^* \rightarrow \pi K$ and $\Delta \rightarrow N\pi$.

Figure 2 shows pseudorapidity distribution of charged hadrons and transverse momentum distribution of negatively charged hadrons. Preliminary experimental data in the pseudorapidity distribution are taken from the PHOBOS collaboration [5]. Experimental data in the k_T distribution are taken from the STAR collaboration [6]. Our results reproduce the experimental data well.

The parameter set in table 1 tells us that the energy density is not extremely high but sufficient for the QGP production. The value 6.0 GeV/fm³ is only 5% higher than that of SPS, 5.74 GeV/fm³ at the same initial time, $\tau = 1.0$ fm. Our value is smaller than the other calculations [7]. This is due to the different thermalization time and the different initial energy density profile. Major discrepancy between the RHIC and the SPS can be seen in

Analysis of one- and two-particle spectra at RHIC

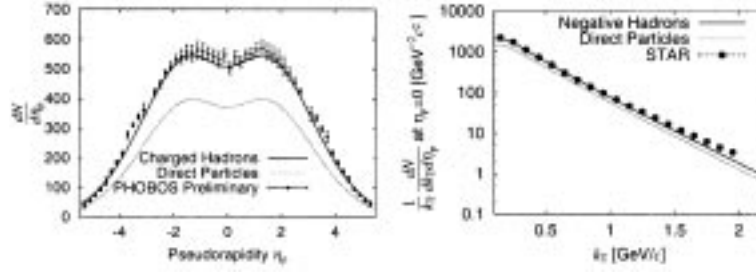


Figure 2. Single-particle spectra at RHIC. Left: Pseudorapidity distribution. Right: Transverse momentum distribution. In both figures, solid lines, dashed lines and symbols denote total number of particles (i.e., including resonance decay), direct components and experimental data, respectively.

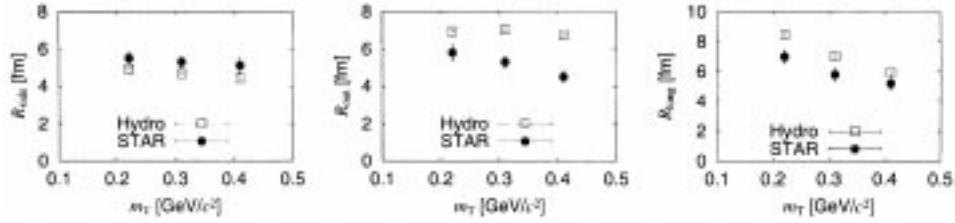


Figure 3. HBT radii at RHIC. From left to right, R_{side} , R_{out} and R_{long} , respectively. Experimental data are taken from the STAR collaboration [8].

the net baryon density and longitudinal extension of the fluid. The net baryon number at the RHIC is much smaller than the one at the SPS. Longitudinal extension along η -axis at the RHIC is twice as large as at the SPS. Hence, much higher colliding energy at the RHIC is converted into the large volume of the hot matter rather than high energy density. We can also see that the transverse flow $v_T = \tanh Y_T$ becomes stronger at the RHIC than at the SPS.

It is well-known as Hanbury–Brown–Twiss effect that one can get the information on the source of particles through two-particle correlation function. Based on the numerical solution of the hydrodynamical equation, we calculate the two-pion correlation functions. Here we consider only the pions directly emitted from the hypersurface, for simplicity. The HBT radii are extracted from the correlation function via a Gaussian fitting function

$$C_{2\text{fit}}(K, q) = 1 + \lambda \exp \left[-R_{\text{out}}^2(K) q_{\text{out}}^2 - R_{\text{side}}^2(K) q_{\text{side}}^2 - R_{\text{long}}^2(K) q_{\text{long}}^2 \right]. \quad (1)$$

Transverse mass dependence of the HBT radii is displayed in figure 3. The sideward HBT radii, R_{side} , show almost consistent result with the experimental data. The outward and longitudinal HBT radii are larger than the experimental data. The outward HBT radii show different behavior with respect to M_T . The experimental result strongly depends on M_T but our result does not show strong dependence on M_T . We also show $R_{\text{out}}/R_{\text{side}}$ which should be a good indicator of the long-lived fluid [9] in figure 4. Our calculation agrees with the SPS data, in which the ratio monotonically increases with K_T . As shown in table 1, our numerical solution of the hydrodynamical equations does not show major difference in

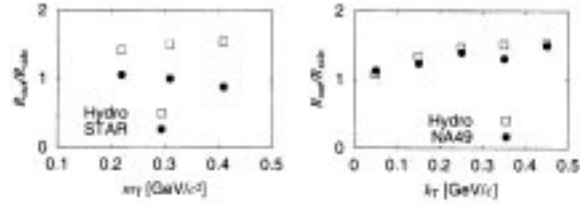


Figure 4. $R_{\text{out}}/R_{\text{side}}$. Left: RHIC. Right: SPS.

lifetime between the RHIC and the SPS because the initial energy density at RHIC is only slightly higher than that at SPS. In fact, the time duration at RHIC is about 6 fm. Hence, the ratio shows similar behavior both qualitatively and quantitatively in our result. However, the experimental result at RHIC clearly decreases with M_T and the value is smaller than our result. For the definite conclusion of this puzzle, we need more and more theoretical investigation.

3. Summary

In summary, we analyze the one-particle distribution and HBT radii based on a hydrodynamical model. Our model successfully reproduce the one-particle distribution at RHIC experiment. The numerical solution shows the QGP production with low net baryon number density and large volume. The maximum energy density is not much higher than the SPS case. HBT radii are also investigated. Our result in figure 3 roughly shows agreement with the experiment. Figure 4 may indicate different particle emission mechanism at RHIC.

Acknowledgements

The author would like to thank I Ohba, H Nakazato, H Nakamura and P Kolb for their helpful discussion and comments. This work is partially supported by Waseda University Grant for Special Research Projects No. 2001A-888 and Waseda University Media Network Center.

References

- [1] Quark Matter 2001, *Proc. Fifteenth Intl. Conf. on Ultra-Relativistic Nucleus–Nucleus Collisions*, (Stony Brook, USA, 14–21 January 2001); *Nucl. Phys.* **A698** (2002)
- [2] T Hirano, K Morita, S Muroya and C Nonaka, *Phys. Rev.* **C65**, 061902(R) (2002) see also references therein
- [3] T Ishii and S Muroya, *Phys. Rev.* **D46**, 5156 (1992)
- [4] C Nonaka, E Honda and S Muroya, *Euro. Phys. J.* **C17**, 663 (2000)
- [5] A Wuosmaa *et al*, PHOBOS Collaboration, in [1]
- [6] C Adler *et al*, STAR Collaboration, *Phys. Rev. Lett.* **87**, 112303 (2001)
- [7] T Hirano, *Phys. Rev.* **C65**, 011901(R) (2002)
- [8] C Adler *et al*, STAR Collaboration, *Phys. Rev. Lett.* **87**, 082301 (2001)
- [9] D H Rischke and M Gyulassy, *Nucl. Phys.* **A608**, 479 (1996)